
A new family of \mathcal{L} -stable block methods with relative measure of stability

Sania Qureshi*

Department of Basic Sciences and Related Studies,
Mehran University of Engineering and Technology,
Jamshoro – 76062, Pakistan

and

Department of Mathematics,
Near East University,
TRNC, Mersin 10, Turkey
Email: sania.qureshi@faculty.muett.edu.pk

*Corresponding author

Amanullah Soomro

Department of Basic Sciences and Related Studies,
Mehran University of Engineering and Technology,
Jamshoro – 76062, Pakistan

Email: soomroamanullah820@gmail.com

Fadugba Sunday Emmanuel

Department of Mathematics,
Faculty of Science,
Ekiti State University,
Ado Ekiti, 360001, Nigeria
Email: sunday.fadugba@eksu.edu.ng

Evren Hincal

Department of Mathematics,
Near East University,
TRNC, Mersin 10, Turkey
Email: evren.hincal@neu.edu.tr

Abstract: There are several nonlinear and stiff mathematical models in fields of science and engineering that have always remained a challenge for numerical analysts and applied mathematicians. Various numerical methods are proposed to deal with stiff models; however, it requires the model to have strong stability characteristics to handle the stiffness in the model. This paper develops a new family of \mathcal{L} -stable block methods with a relative measure of stability for the solution of stiff differential equations with different characteristics. First, the theoretical properties of the proposed block method in terms of local truncation errors, absolute stability, consistency, convergence, and order stars have been analysed and investigated. Then,

seven illustrative stiff differential models have been solved to measure the proposed method's performance, suitability, effectiveness, and efficiency. Finally, the error distributions and the precision factors are computed in the comparison of several existing methods having similar properties as that of the proposed \mathcal{L} -stable block method.

Keywords: stiff systems; \mathcal{A} -stability; local error; order stars; implicit stiff solver; efficiency curves.

Reference to this paper should be made as follows: Qureshi, S., Soomro, A., Emmanuel, F.S. and Hincal, E. (2022) 'A new family of \mathcal{L} -stable block methods with relative measure of stability', *Int. J. Applied Nonlinear Science*, Vol. 3, No. 3, pp.197–222.

Biographical notes: Sania Qureshi completed her PhD in 2019 from University of Sindh. During her PhD studies, she was awarded two scholarships under which she visited Division of Mathematics, University of Dundee, Scotland, UK in 2016 and Institute of Computational Mathematics, Technische Universitaet Braunschweig, Germany in 2018. She has several publications on mathematical epidemiology, fractional calculus, and numerical techniques for ODEs. Since 2008, she is the full-time faculty member at Mehran University of Engineering and Technology, Pakistan.

Amanullah Soomro graduated from Institute of Mathematics and Computer Sciences, University of Sindh, Jamshoro with BS degree in 2019. Nowadays, he is pursuing his MPhil Research Studies from the Department of Basic Sciences and Related Studies at Mehran University of Engineering and Technology, Jamshoro, Sindh, Pakistan. He is a co-author of four research papers recently published in Scopus international journals. At the same time, he is serving as a teaching assistant in the same department.

Fadugba Sunday Emmanuel is currently working at the Department of Mathematics, Ekiti State University, Ado Ekiti as a Senior Lecturer. He does his research in financial mathematics, stochastic analysis with applications, numerical analysis, solutions to fractional differential equations, algebra and applied mathematics.

Evren Hincal completed his PhD at the Eastern Mediterranean University with the cooperation of Imperial College in 1991. Between 2000–2001, he visited Imperial College and he worked with Neurobiology Group on the cancer epidemiology. He has several publications about cancer statistics, cancer epidemiology and mathematical modelling about cancer in refereed international journals. Since 2007, he is a full-time member of Near East University Department of Mathematics.

1 Introduction

As per the scientific survey, the need for numerical methods with strong stability characteristics to deal with nonlinear, stiff, singular, and singularly perturbed models is on the rise. Based on which the present study has been carried out to develop a

new family of \mathcal{L} -stable block numerical methods having consistency, accuracy, stability (particularly, \mathcal{L} -stability), and convergence. The new method is equally applicable to systems of ODEs as demonstrated. Comparison with a family of Radau type methods and some block ones having an order of convergence larger than one developed in the manuscript shows the latter's superiority when tested upon various differential models chosen from several fields of studies. In addition, this manuscript expands on the prior research works as given in Skwame et al. (2012) and Akinfenwa et al. (2018).

The initial value problems (IVPs) in ordinary differential equation (ODEs) of the following form are the most frequently used problems in several fields of science and engineering:

$$\begin{aligned} v'(x) &= g(x, v(x)), v(x_0) = v_0, \\ v : I &\rightarrow \mathbb{R}^n \text{ and } g : I \times \mathbb{R}^n \rightarrow \mathbb{R}^n \text{ with } I = [x_0, X_N], \end{aligned} \quad (1)$$

where v_0 represents the value of v at $x = x_0$ and g is a continuously differentiable function that satisfies Lipschitz's condition and thus the given problem confirms the existence of unique solution as described in Henrici (1962).

Many scholars in the field of numerical analysis have been working on problems of the type (1) because these problems are commonly used to represent several real-life situations. There are various applications of equation (1) in dynamic systems, electrical networks, logistic growth, trajectory of a particle, and many more (Kandasamy et al., 2005; Awoyemi, 2001). Numerous problems in the fields of mathematics, engineering, computer science, and the physical sciences, such as mechanics, neuroscience, planetary chemistry, and environmental sciences have been solved using numerical integrators and modern high-speed electronic computers. There are other models, such as the SIR model and Prothero Robinson oscillatory problem, highly stiff oscillatory problems, and other related problems may all be represented in the form of a scalar equation or a first-order system, as in equation (1). It is usually accepted that many first-order ODEs of the type (1) do not have accurate solutions; therefore, numerical approximations are required. A large number of scholars have used various ways to provide numerical answers to the problem in equation (1), particularly the well-known multistep and Runge-Kutta methods. Among them are Lambert (1991), Hairer et al. (2008, 1993), Butcher (2016), Gragg and Stetter (1964), Skwame et al. (2012), Akinfenwa et al. (2018), Qureshi and Ramos (2018), Qureshi and Yusuf (2020) and Fadugba (2020) to mention a few. The main disadvantage of these approaches is their high computational cost, which has an effect on the overall performance of the methods. Researchers have developed numerical methods suitable for a particular kind of ODE based on several types of ODEs, including nonlinear, autonomous, non-autonomous, stiff, singular, and singularly perturbed. A fully sixth-order implicit block backward differentiation formula with two off-step points (BBDFO(6)), for the integration of first-order ODEs that exhibit stiffness, was proposed by Nasarudin et al. (2020). An almost \mathcal{L} -stable BDF-type method for the numerical solution of stiff ODEs arising from the method of lines was proposed by Ramos and Vigo-Aguiar (2007). Rufai and Ramos (2020) developed a one-step hybrid block method for solving boundary value problems, which was used to solve classical one-dimensional Bratu's and Troesch's problems. They also investigated the convergence analysis of the new technique, and also considered some improving strategies to get better performance of the method. An implicit two-step hybrid block method based on collocation and interpolation techniques for the solution of linear

and nonlinear third-order boundary value problems in ODEs was proposed by Ramos and Rufai (2020). See et al. (2014) proposed a three-step block method of Adam's type to solve nonlinear second-order two-point boundary value problems of Dirichlet type and Neumann type directly. They also extended the proposed method for the solution of the system of second-order boundary value problems with the same or different two boundary conditions. Abdulganiy et al. (2021) constructed a functionally fitted method via interpolating function consisting both trigonometric and exponential types to solve first-order differential systems whose solutions present an oscillatory behaviour with better accuracy. A hybrid second-derivative three-step method of order seven generated from a single continuous scheme via interpolation and collocation procedures for solving first order stiff differential equations was derived and proposed by Akinfenwa et al. (2020). A new family of block methods known as self-starting second-derivative Simpson's type (SDSM) of uniform order $p = 2k + 2$ for step number $k \leq 6$ to solve system of stiff ODEs was successfully developed by Awari et al. (2020). Ajayi et al. (2019), Qureshi et al. (2021), Shokri et al. (2020) and Shokri et al. (2020) presented a family of stiffly stable (\mathcal{A} -stable, \mathcal{L} -stable, P -stable and $\mathcal{A}(\alpha)$ -stable second-derivative block methods (SDBMs) capable of solving first-order stiff ODEs. Singla et al. (2021) and Ramos et al. (2021) considered an adaptive step-size formulation of an optimised block method of embedded-type procedure for directly solving general second-order IVPs of ODEs numerically. Sunday et al. (2015) developed a two-step hybrid block method for the solution of stiff and oscillatory first-order ODEs. They derived the method using the Laguerre polynomial as a basis function via interpolation and collocation techniques. Ramos (2017) presented a two-step block method of hybrid type obtained from a continuous approximation derived via interpolation and collocation at different points for the direct solution of general first-order initial-value problems in ODEs. Other applications and numerical methods with new approaches can be found in Aliev et al. (2020, 2021), Argyros and George (2021), Gao et al. (2021), Rao and Kalyani (2021), Heydari (2020), Mostafa and El Hawsh (2020), Khalsaraei and Shokri (2020), Ashyralyev et al. (2020), Achchab et al. (2020), Iskenderov et al. (2016), Musaev (2021), Onyejekwe (2018), Kumar and Verma (2021), Jena et al. (2022) and Bavi et al. (2022). According to Lambert (1991), Nasarudin et al. (2020) and Wanner and Hairer (1996), the IVP in equation (1) is said to be stiff in nature if it contains widely varying time scales, i.e., some components of the solution decay much more rapidly than others; the step size is dictated by the stability requirements rather than the accuracy requirements; and explicit methods do not work, or work only extremely slowly.

The present paper derives a new family of \mathcal{L} -stable block methods with relative measure of stability for the solution of equation (1).

The rest of the paper is outlined as follows: Section 2 presents the mathematical formulation. Section 3 captures the theoretical analysis. Section 4 compares the numerical simulations of the proposed \mathcal{L} -stable block method with several existing methods designed to deal with the stiff differential models. Concluding remarks with future plans are presented in Section 5.

2 Mathematical formulation

The purpose of this section is to develop a second-derivative one-step block method with \mathcal{L} -stability for solving the problems of type (1). It may be noted that the reason to take second-derivative is to basically obtain the \mathcal{L} -stable block method. The property of \mathcal{L} -stability is considered to be a favourable property to solve stiff differential models. We assume $n = 1$ in equation (1) to simplify the method's derivation. At later stage, the derived method will also be made applicable to solve stiff and non-stiff systems while using the component-wise approach. The local approximate solution $v(x)$ is initially assumed in the form of a polynomial basis $p(x)$ over a generic sub-interval $[x_n, x_{n+1}]$, where $x_{n+1} = x_n + \Delta x$ and Δx is the step-size.

$$v(x) \approx p(x) = \sum_{j=0}^5 \phi_j x^j, \tag{2}$$

where the symbol $\phi_j \in \mathbb{R}$ stands for real unknown parameters. Double differentiation of equation (2) produces the following results:

$$v'(x) \approx p'(x) = \sum_{j=1}^5 j\phi_j x^{j-1}, \tag{3}$$

$$v''(x) \approx p''(x) = \sum_{j=2}^5 j(j-1)\phi_j x^{j-2}. \tag{4}$$

Consider two intra-step points, $x_{n+r} = x_n + r\Delta x, x_{n+s} = x_n + s\Delta x$ with $0 < r < s < 1$, to compute the approximate solution of the IVP (1) at the point x_{n+1} , assuming that $v_n = v(x_n)$. To start the procedure, consider the approximation in equation (2) determined at x_n , and its first-order derivative determined at the points $x_n, x_{n+r}, x_{n+s}, x_{n+1}$. By so doing, we obtain the following linear system of six equations in six real unknown parameters $\phi_j, j = 0, 1, \dots, 5$:

$$\begin{pmatrix} 1 & x_n & x_n^2 & x_n^3 & x_n^4 & x_n^5 \\ 0 & 1 & 2x_n & 3x_n^2 & 4x_n^3 & 5x_n^4 \\ 0 & 1 & 2x_{n+r} & 3x_{n+r}^2 & 4x_{n+r}^3 & 5x_{n+r}^4 \\ 0 & 1 & 2x_{n+s} & 3x_{n+s}^2 & 4x_{n+s}^3 & 5x_{n+s}^4 \\ 0 & 1 & 2x_{n+1} & 3x_{n+1}^2 & 4x_{n+1}^3 & 5x_{n+1}^4 \\ 0 & 0 & 2 & 6x_{n+1} & 12x_{n+1}^2 & 20x_{n+1}^3 \end{pmatrix} \begin{pmatrix} \phi_0 \\ \phi_1 \\ \phi_2 \\ \phi_3 \\ \phi_4 \\ \phi_5 \end{pmatrix} = \begin{pmatrix} v_n \\ g_n \\ g_{n+r} \\ g_{n+s} \\ g_{n+1} \\ \gamma_{n+1} \end{pmatrix}. \tag{5}$$

Solving the above linear system gives values of the six unknown coefficients $\phi_j, j = 0, 1, \dots, 5$ which are not shown here for brevity. Putting these values in equation (2) while using the change of variable $x = x_n + t\Delta x$, we reach the following:

$$p(x_n + t\Delta x) = \phi_0 g_n + \Delta x \left(\eta_0 g_n + \eta_r g_{n+r} + \eta_s g_{n+s} + \eta_1 g_{n+1} \right) + \Delta x^2 (\zeta_1 \gamma_{n+1}), \tag{6}$$

where

$$\begin{aligned}
 \phi_0 &= 1, \\
 \eta_0 &= \frac{(3/5 t^4 + (-3/4 r - 3/4 s - 3/2) t^3 + ((s + 2) r + 2 s + 1) t^2 + ((-3 s - 3/2) r - 3/2 s) t + 3 s r) \Delta t}{3 s r}, \\
 \eta_r &= -\frac{\Delta x t^2 (15 s t^2 - 12 t^3 - 40 s t + 30 t^2 + 30 s - 20 t)}{60 (r - 1)^2 (r - s)}, \\
 \eta_s &= \frac{\Delta x t^2 (15 r t^2 - 12 t^3 - 40 r t + 30 t^2 + 30 r - 20 t)}{60 (s - 1)^2 (r - s)}, \\
 \eta_1 &= -\frac{\Delta x t^2 (t (5 r^2 (4 s^2 - 3 s t + 6 (t - 2)) + r (-15 s^2 t + 6 s (2 t^2 + 5 t - 10) - 24 t^2 + 80) + 30 s^2 (t - 2) + s (80 - 24 t^2) + 12 t (3 t - 5)) - 60 r s (r (s - \frac{3}{2}) - \frac{3 s}{2} + 2))}{60 (r - 1)^2 (s - 1)^2}, \\
 \zeta_1 &= \frac{\Delta x^2 t^2 (20 r s t - 15 r t^2 - 15 s t^2 + 12 t^3 - 30 s r + 20 r t + 20 s t - 15 t^2)}{(60 s - 60) (r - 1)}.
 \end{aligned} \tag{7}$$

To get the one-step block method, we evaluate $p(x_n + t\Delta x)$ at the collocation points x_{n+r}, x_{n+s} , and x_{n+1} , that is, we take $x = r, s, 1$. This results in the linear system containing three equations as shown below:

$$\begin{aligned}
 v_{n+r} &= \frac{\Delta x^2 r^2 (-3 r^3 + 5 r^2 s + 5 r^2 - 10 s r) \gamma_{n+1}}{(60 s - 60) (r - 1)} \\
 &+ \left(\frac{(-3 r^4 + 5 r^3 s + 10 r^3 - 20 r^2 s - 10 r^2 + 30 s r) g_n}{60 s} \right. \\
 &- \frac{r (-12 r^3 + 15 r^2 s + 30 r^2 - 40 s r - 20 r + 30 s) g_{n+r}}{60 (r - 1)^2 (r - s)} \\
 &+ \frac{r^2 (3 r^3 - 10 r^2 + 10 r) g_{n+s}}{60 (s - 1)^2 (r - s) s} \\
 &\left. - \frac{r^2 (-3 r^4 s + 5 r^3 s^2 + 6 r^4 + 6 r^3 s - 30 s^2 r^2 - 24 r^3 + 30 r^2 s + 30 r s^2 + 20 r^2 - 40 s r) g_{n+1}}{60 (s - 1)^2 (r - 1)^2} \right) \Delta x + v_n,
 \end{aligned} \tag{8}$$

$$\begin{aligned}
 v_{n+s} = & \frac{\Delta x^2 s^2 (5rs^2 - 3s^3 - 10sr + 5s^2) \gamma_{n+1}}{(60s - 60)(r - 1)} \\
 & + \left(\frac{(5rs^3 - 3s^4 - 20rs^2 + 10s^3 + 30sr - 10s^2) g_n}{60r} \right. \\
 & - \frac{s^2 (3s^3 - 10s^2 + 10s) g_{n+r}}{60(r - 1)^2 (r - s)r} \\
 & + \frac{s(15rs^2 - 12s^3 - 40sr + 30s^2 + 30r - 20s) g_{n+s}}{60(s - 1)^2 (r - s)} \\
 & \left. - \frac{s^2 (5r^2s^3 - 3rs^4 - 30s^2r^2 + 6rs^3 + 6s^4 + 30r^2s) + 30rs^2 - 24s^3 - 40sr + 20s^2) g_{n+1}}{60(s - 1)^2 (r - 1)^2} \right) \Delta x + v_n,
 \end{aligned} \tag{9}$$

$$\begin{aligned}
 v_{n+1} = & \frac{\Delta x^2 (-10rs + 5r + 5s - 3) \gamma_{n+1}}{(60s - 60)(r - 1)} + \left(\frac{(20rs - 5r - 5s + 2) g_n}{60rs} \right. \\
 & - \frac{(5s - 2) g_{n+r}}{60(r - 1)^2 (r - s)r} + \frac{(5r - 2) g_{n+s}}{60(s - 1)^2 (r - s)s} \\
 & \left. - \frac{(-40r^2s^2 + 75r^2s + 75rs^2 - 30r^2 - 138rs - 30s^2 + 56r + 56s - 24) g_{n+1}}{60(s - 1)^2 (r - 1)^2} \right) \Delta x + v_n.
 \end{aligned} \tag{10}$$

We have several choices for the two parameters over the block $[0, 1]$ and for each choice, there will be a new implicit method that can be considered a member of the entire family of methods. We have arbitrarily chosen two values $r = \frac{1}{5}$ and $s = \frac{2}{3}$ and therefore obtained one of the new members of the family as given below:

$$\begin{aligned}
 v_{n+r} = & -\frac{8\Delta x^2 \gamma_{n+1}}{3,125} \\
 & + \left(\frac{5,941 g_n}{75,000} + \frac{163 g_{n+r}}{1,200} - \frac{783 g_{n+s}}{25,000} + \frac{2,441 g_{n+1}}{150,000} \right) \Delta x + v_n, \\
 v_{n+s} = & \frac{\Delta x^2 \gamma_{n+1}}{81} + \left(\frac{g_n}{27} + \frac{125 g_{n+r}}{324} + \frac{g_{n+s}}{3} - \frac{29 g_{n+1}}{324} \right) \Delta x + v_n, \\
 v_{n+1} = & \left(\frac{g_n}{24} + \frac{125 g_{n+r}}{336} + \frac{27 g_{n+s}}{56} + \frac{5 g_{n+1}}{48} \right) \Delta x + v_n.
 \end{aligned} \tag{11}$$

Using the extended Butcher Tableau, the newly formulated strategy as given in equation (11) can be presented in the form of coefficients and considered to be a new implicit block RK type method as follows:

$$\begin{array}{c|c}
 c & \mathcal{A} \\
 \hline
 & \hat{\mathcal{A}} \\
 \hline
 b^T & \hat{b}^T
 \end{array}$$

The structure given above is rewritten as follows:

0	0	0	0	0	0	0	0	0
$\frac{1}{5}$	$\frac{5,941}{75,000}$	$\frac{163}{1,200}$	$\frac{-783}{25,000}$	$\frac{2,441}{150,000}$	0	0	0	$-\frac{8}{3,125}$
$\frac{2}{3}$	$\frac{1}{27}$	$\frac{125}{324}$	$\frac{1}{3}$	$\frac{-29}{324}$	0	0	0	$-\frac{1}{81}$
1	$\frac{1}{24}$	$\frac{125}{336}$	$\frac{27}{56}$	$\frac{5}{48}$	0	0	0	0
	$\frac{1}{24}$	$\frac{125}{336}$	$\frac{27}{56}$	$\frac{5}{48}$	0	0	0	0

3 Theoretical analysis

This section is designed to present abstract characteristics of the proposed block method given in equation (11). These characteristics include analysis of the local truncation errors, consistency, zero-stability, linear stability, convergence, and relative measure of stability (order stars).

3.1 Local truncation error and consistency

The one-step optimised block method given in equation (11) can be rewritten using the matrix notation as follows:

$$\mathcal{I}^0 V_{n+1} = \mathcal{C}^1 V_n + \Delta x (\mathcal{D} G_{n+1} + \mathcal{B}^0 G_n + \Delta x \mathcal{B}^1 \bar{G}_{n+1}), \tag{12}$$

where \mathcal{I}^0 , \mathcal{B}^0 , \mathcal{C}^1 , \mathcal{D} , and \mathcal{B}^1 stand for 3×3 matrices as given below

$$\mathcal{I}^0 = \begin{bmatrix} 1 & 0 & 0 \\ 0 & 1 & 0 \\ 0 & 0 & 1 \end{bmatrix}, \quad \mathcal{C}^1 = \begin{bmatrix} 0 & 0 & 1 \\ 0 & 0 & 1 \\ 0 & 0 & 1 \end{bmatrix}, \quad \mathcal{B}^0 = \begin{bmatrix} 0 & 0 & \frac{5,941}{75,000} \\ 0 & 0 & \frac{1}{27} \\ 0 & 0 & \frac{1}{24} \end{bmatrix}, \tag{13}$$

$$\mathcal{B}^1 = \begin{bmatrix} 0 & 0 & \frac{-8}{3,125} \\ 0 & 0 & \frac{1}{81} \\ 0 & 0 & 0 \end{bmatrix}, \quad \mathcal{D} = \begin{bmatrix} \frac{163}{1,200} & \frac{-783}{25,000} & \frac{2441}{150,000} \\ \frac{125}{324} & \frac{1}{3} & \frac{-29}{324} \\ \frac{125}{336} & \frac{27}{56} & \frac{5}{48} \end{bmatrix}, \tag{14}$$

and

$$\begin{aligned}
 V_n &= (v_{n-1+r}, v_{n-1+s}, v_n)^T, \\
 V_{n+1} &= (v_{n+r}, v_{n+s}, v_{n+1})^T, \\
 G_n &= (g_{n+r}, g_{n+s}, g_n)^T, \\
 G_{n+1} &= (g_{n+r}, g_{n+s}, g_{n+1})^T, \\
 \tilde{G}_{n+1} &= (\gamma_{n+r}, \gamma_{n+s}, \gamma_{n+1})^T.
 \end{aligned}
 \tag{15}$$

We assume an associated linear operator χ for each of the formulas computed in equation (11) as given below:

$$\begin{aligned}
 \chi[J(x); \Delta x] &= \sum_{k=0, r, s, 1} [\tilde{\gamma}_k J(x_n + k\Delta x) - \Delta x \tilde{\eta}_k J'(x_n + k\Delta x) \\
 &\quad - \Delta x^2 \tilde{\eta}_k J''(x_n + k\Delta x)],
 \end{aligned}
 \tag{16}$$

for $i = r, s, 1$, where $v(x)$ represents an arbitrary analytic function in the neighbourhood of x_n , and G_i corresponds to the right-hand sides of the each formula given in equation (11) after the approximate values have been replaced with the exact values.

Definition 3.1: The difference operator in equation (16) and the corresponding associated formulas of equation (11) are said to have order r if $\chi_0 = \chi_1 = \dots = \chi_r = 0, \chi_{r+1} \neq 0$, where χ_r is the coefficient of the power Δx^i in the Taylor series expansion of equation (16) as mentioned in Ramos and Rufai (2018).

After expanding the terms in equation (16) in Taylor series about the point x_n in powers of Δx while assuming that $v(x)$ is sufficiently differentiable, we obtain the order ($r = 5$) and the local truncation error of the main formula as follows

$$\chi(v(x_{n+1}); \Delta x) = -\frac{(\Delta x)^6}{108,000} \frac{d^6}{dx_n^6} v(x_n) + \mathcal{O}(\Delta x^7).
 \tag{17}$$

The local truncation error determined above shows fifth-order accuracy of the proposed block method (11), hence the method is considered to be consistent (see Rufai et al., 2016).

3.2 Zero-stability and convergence

Zero stability is a kind of stability issue concerned with the behaviour of the difference system in equation (12) when $\Delta x \rightarrow 0$. For $\Delta x \rightarrow 0$, the method in equation (12) gives the system of equations

$$v_{n+r} = v_n, \quad v_{n+s} = v_n, \quad v_{n+1} = v_n,
 \tag{18}$$

which may be rewritten using the matrix formalism as $\mathcal{I}^0 V_n - \mathcal{C}^1 V_{n+1} = 0$, with V_n, V_{n-1} and \mathcal{C}^1 as before, and \mathcal{I}^0 shows the identity matrix of the third-order. The proposed block method is said to be zero stable when the roots λ_j of the

first characteristic polynomial $\Omega(\lambda)$ given by $\Omega(\lambda) = |\mathcal{I}^0\lambda - \mathcal{C}^1|$ satisfy $|\lambda_j| \leq 1$, and for those roots with $|\lambda_j| = 1$ the corresponding multiplicity does not exceed 1 [see the work of Lambert (1973)]. Since $\Omega(\lambda) = \lambda^2(\lambda - 1)$, the proposed block method in equation (12) is zero stable. As discussed by Henrici (1962), the convergence of the proposed block method given in equation (11) can be claimed since zero-stability+consistency = convergence.

3.3 Linear stability

As we discussed earlier, zero-stability is a concept concerning the behaviour of the numerical method for the step-size $\Delta x > 0$. In order to determine whether a numerical method will produce reasonable results with a given value of $\Delta x > 0$, we need a notion of stability that is different from zero-stability. In most numerical methods intended for solving first-order problems, the linear stability properties are usually analysed by considering the linear equation given by the Dahlquist's test equation $v' = \sigma v(x)$ for $Re(\sigma) < 0$. Zero-stability depends just on the method but linear stability, in general for finite $\Delta x > 0$, depends on the problem also. We will determine the region in which the numerical method reproduces the behaviour of the true solutions for the test equation. After applying the method in equation (11) to the Dahlquist's test equation, we obtain the following recurrence equation:

$$V_{n+1} = \mathcal{M}(z)V_n, \quad z = \sigma\Delta x, \quad (19)$$

where σ is a complex parameter and $\mathcal{M}(z)$ is known as the stability matrix of the numerical method, which can be expressed as:

$$\mathcal{M}(z) = (\mathcal{I}^0 - z\mathcal{D} - z^2\mathcal{B}^1)^{-1}(\mathcal{C}^1 + z\mathcal{B}^0), \quad (20)$$

with $\mathcal{B}^0, \mathcal{B}^1, \mathcal{C}^1$, and \mathcal{D} as defined before. The stability matrix $\mathcal{M}(z)$ in equation (20) has the eigenvalues

$$\left(0, 0, \frac{4z^3 + 63z^2 + 384z + 900}{z^4 - 17z^3 + 129z^2 - 516z + 900} \right).$$

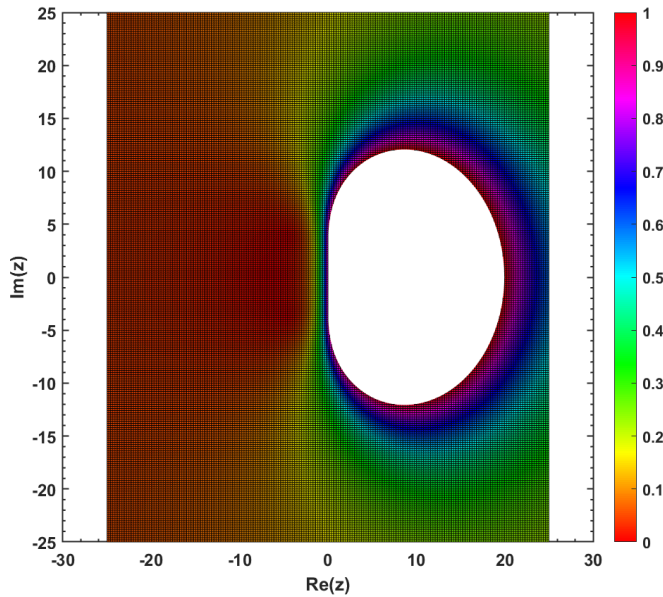
We notice whether that the stability of the approximate solution depends on the eigenvalues computed above, and the stability features of the proposed block method will be characterised by the spectral radius, $\rho(\mathcal{M}(z))$. The absolute stability area \mathcal{S} is given as $\mathcal{S} = \{z \in \mathbb{C} : |\rho(\mathcal{M}(z))| < 1\}$. The proposed method's stability region is shown in Figure 1, where the entire left-half complex plane is covered. This proves method's \mathcal{A} -stability. Furthermore, the proposed method is \mathcal{L} -stable, since $\rho(\mathcal{M}(z)) \rightarrow 0$ for $z \rightarrow \infty$. It is worthwhile to mention that the \mathcal{L} -stable methods are found to be promising candidates for solving stiff

3.4 Relative measure of stability

The relative measure of stability also known as the order stars are a powerful modern tool for numerical methods. In a consistent framework, they provide critical information such as order and stability conditions for the underlying numerical method. For the

proposed \mathcal{L} -stable block method (11), we had $\rho(\mathcal{M}(z))$ given by a rational approximate. This type of approximate has further attractive qualities. An order star can be used to investigate the properties of a relative approximation in the complex plane. It is important to remember that the study of approximate characteristics frequently arises from our interest in a numerical method.

Figure 1 The plot of the absolute stability region for the \mathcal{L} -stable block method given in equation (11) (see online version for colours)



Let \mathcal{P} and \mathcal{Q} be possibly complex-valued polynomials of degree m and n , respectively, and denote the quotient $\mathcal{R}(z) = \mathcal{P}/\mathcal{Q}$ by \mathcal{R}_m^n . Certainly, a zero of \mathcal{Q} is a pole of the rational function $\mathcal{R}(z)$. Let $\mathcal{F}(z)$ be a complex function. An order star $\varrho(z)$ defines a partition in the complex plane, namely the triplet $\{\mathcal{U}_+, \mathcal{U}_0, \mathcal{U}_-\}$, where

$$\begin{aligned} \mathcal{U}_+ &= \{z : \varrho(z) > \xi\}, \\ \mathcal{U}_0 &= \{z : \varrho(z) = \xi\}, \\ \mathcal{U}_- &= \{z : \varrho(z) < \xi\}. \end{aligned} \tag{21}$$

Fundamentally, there are two types of order stars, $\varrho(z)$, that are usually considered in the literature as follows:

$$|\mathcal{R}(z)/\mathcal{F}(z)| \text{ with } \xi = 1, \text{ and } \operatorname{Re}(\mathcal{R}(z) - \mathcal{F}(z)) \text{ with } \xi = 0. \tag{22}$$

Some of the properties related to the order stars are stated below:

Property 3.2: (Order) $\mathcal{R}(z)$ is an order q approximation to $\exp(z)$ if z is connected by $q + 1$ parts of \mathcal{U}_+ and divided by $q + 1$ parts of \mathcal{U}_+ . With an asymptotic angle of $(\frac{\pi}{q+1})$, all parts approach z .

Bounded, related parts of \mathcal{U}_+ are commonly referred to as fingers, whereas similar sections of \mathcal{U}_- are referred to as dual fingers.

Property 3.3: (Enumeration) The number of \mathcal{R} poles (zeros) in each bounded linked part of \mathcal{U}_+ (\mathcal{U}_-), multiplied by their multiplicity, equals the number of interpolation points (i.e., such that $\mathcal{R}(z) = \mathcal{F}(z)$).

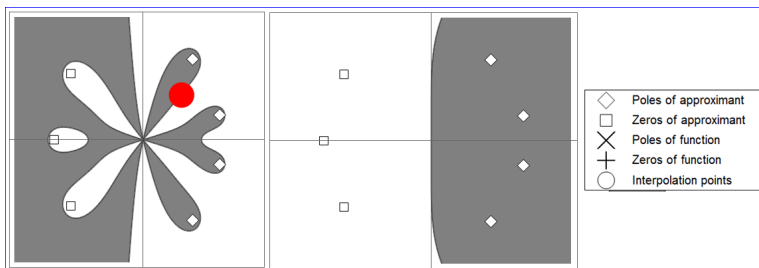
Property 3.4: (Unbounded) There are two unbounded associated parts, one of (\mathcal{U}_+) and the other of (\mathcal{U}_-).

It is common practice to differentiate \mathcal{U}_+ from \mathcal{U}_- by shading the former. By doing so, it becomes clear that the region of growth of relative stability is shown for the set denoted by \mathcal{U}_+ while, the region of contractivity lies under the set \mathcal{U}_- . As a result, the boundary between the relative stability region and the region of contractivity is determined with \mathcal{U}_0 . A set of the following three regions is obtained can be considered by redefining the order star of $\rho(\mathcal{M}(z))$. Since our major concern is the first type of order stars, therefore we obtain the following sets:

$$\begin{aligned} \mathcal{U}_+ &= \{z \in \mathbb{C} : |\rho(\mathcal{M}(z))| > |\exp(z)|\} = \{z \in \mathbb{C} : |\exp(-z)\rho(\mathcal{M}(z))| > 1\}, \\ \mathcal{U}_0 &= \{z \in \mathbb{C} : |\rho(\mathcal{M}(z))| = |\exp(z)|\} = \{z \in \mathbb{C} : |\exp(-z)\rho(\mathcal{M}(z))| = 1\}, \\ \mathcal{U}_- &= \{z \in \mathbb{C} : |\rho(\mathcal{M}(z))| < |\exp(z)|\} = \{z \in \mathbb{C} : |\exp(-z)\rho(\mathcal{M}(z))| < 1\}. \end{aligned}$$

The graphs of above sets yield some star-like (fingers) different from the one we are familiar with (regions of absolute stability). In Figure 2, order stars are shown for the proposed \mathcal{L} -stable block method (11) where the shaded regions are for \mathcal{U}_+ . It may also be noted that the intersection of \mathcal{U}_+ with the imaginary axis is a null set including no poles in the region where $Re(z) < 0$. It represents \mathcal{A} -acceptable phenomena for the rational stability function $\rho(\mathcal{M}(z))$ or the proposed \mathcal{L} -stable block method (11) with $z = \sigma \Delta x$.

Figure 2 The plot of the order stars and the absolute stability region for the \mathcal{L} -stable block method given in equation (11), obtained as a relative comparison with 1 (see online version for colours)



4 Numerical simulations

This section discusses the numerical simulations of the proposed \mathcal{L} -stable block method given in equation (11) on the basis of accuracy via error distributions (absolute

maximum global error = $\max_{1 \leq n \leq N} \|v(x_n) - v_n\|$, absolute error computed at the last mesh point over the chosen integration interval = $\|v(x_N) - v_N\|$, norm = $\sqrt{\sum_{1 \leq n \leq N} (v(x_n) - v_n)^2}$, and root mean square error = $\sqrt{\frac{1}{N} \sum_{1 \leq n \leq N} (v(x_n) - v_n)^2}$, precision factor (scd = $-\log_{10} \|v(x_N) - v_N\|_\infty$), and time-efficiency (CPU time measured in seconds). Several numerical experiments are chosen in the form of stiff differential models and subsequently solved with the proposed method including following methods for the comparative analysis:

- \mathcal{L} -stable: Proposed fifth-order block method given in equation (11).
- MHIRK: Multi-derivative hybrid implicit Runge-Kutta method appeared in Akinfenwa et al. (2018).
- RadauI, RadauIIA and IRK: Fully-implicit RK type fifth-order methods appeared in Butcher (2016). The Radau family is frequently used for solving stiff differential systems.
- BSHM1 and BSHM2: \mathcal{L} -stable block hybrid Simpson’s methods appeared in Skwame et al. (2012).
- Laguerre: Laguerre polynomial hybrid block method of at least fifth-order convergence appeared in Sunday et al. (2015).

Problem 1: A highly stiff IVP taken from Yu (2004) is given as follows:

$$v'(x) = -\varepsilon[v(x) - \exp(-x)] - \exp(-x), v(0) = 0, \tag{23}$$

whose exact solution is: $v(x) = \exp(-x) - \exp(-\varepsilon x)$, where $\varepsilon = 10^3$.

Table 1 The error distributions and the precision factor (scd) for Problem 1 with number of steps = 10^2

	<i>MaxErr</i>	<i>LastErr</i>	<i>Norm</i>	<i>RMSE</i>	<i>scd</i>
L-stable	9.209×10^{-4}	1.122×10^{-20}	9.210×10^{-4}	9.164×10^{-5}	3.036
RadauIIA	1.869×10^{-2}	2.064×10^{-13}	1.870×10^{-2}	1.860×10^{-3}	1.728
MHIRK	2.837×10^{-3}	2.179×10^{-20}	2.838×10^{-3}	2.823×10^{-4}	2.547
BSHM1	9.055×10^{-2}	6.434×10^{-18}	9.675×10^{-2}	9.533×10^{-3}	1.043
BSHM2	2.702×10^{-1}	3.973×10^{-14}	2.875×10^{-1}	2.833×10^{-2}	0.568
IRK	2.515×10^{-1}	3.928×10^{-10}	2.608×10^{-1}	2.595×10^{-2}	0.599
RadauI	8.517×10^{-2}	4.317×10^{-13}	8.539×10^{-2}	8.497×10^{-3}	1.070
Laguerre	4.574×10^{-2}	2.333×10^{-18}	4.756×10^{-2}	4.732×10^{-3}	1.340

The stiff IVP (23) is simulated over the integration interval $[0, 0.5]$ while taking different number of steps in powers of 10. The numerical results are shown in Tables 1–3 wherein computations for the accuracy and the precision factor are carried out with the proposed and several other methods. It can be seen that the proposed \mathcal{L} -stable method performs better in both directions, namely, smallest errors and highest precision factors are achieved with the method given in equation (11). The fifth-order accuracy is also observed from the behaviour of last absolute error since the powers of 10 decrease by magnitude 5 with every 1 order of magnitude increase in the powers of 10 in number

of steps. The methods IRK and Radaul diverge for this stiff IVP as shown by the computation of error distributions but maximum absolute global error whereas BSHM2 method does not converge for $n = 100$. Moreover, the efficiency curve given in Figure 3 reveals time-efficiency of the proposed \mathcal{L} -stable method wherein the method RadaulIA is observed to be the most expensive one.

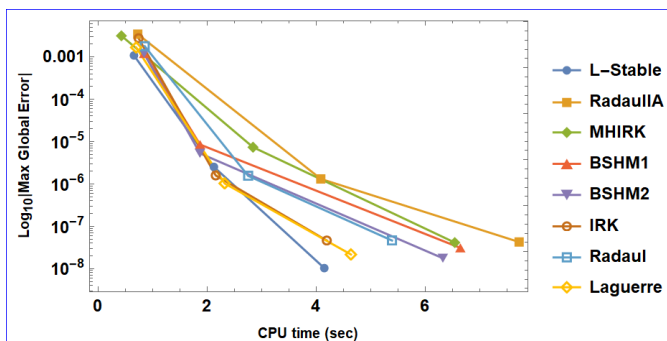
Table 2 The error distributions and the precision factor (scd) for Problem 1 with number of steps = 10^3

	<i>MaxErr</i>	<i>LastErr</i>	<i>Norm</i>	<i>RMSE</i>	<i>scd</i>
L-stable	9.813×10^{-8}	1.629×10^{-25}	1.882×10^{-7}	5.950×10^{-9}	7.008
RadaulIA	1.482×10^{-6}	3.748×10^{-18}	2.844×10^{-6}	8.989×10^{-8}	5.829
MHIRK	2.626×10^{-7}	4.475×10^{-25}	5.037×10^{-7}	1.592×10^{-8}	6.581
BSHM1	5.667×10^{-5}	1.164×10^{-23}	6.362×10^{-5}	2.009×10^{-6}	4.247
BSHM2	4.122×10^{-5}	8.793×10^{-20}	5.921×10^{-5}	1.870×10^{-6}	4.385
IRK	1.805×10^{-6}	1.834×10^{-15}	3.463×10^{-6}	1.095×10^{-7}	5.744
Radaul	1.759×10^{-6}	4.141×10^{-18}	3.375×10^{-6}	1.067×10^{-7}	5.755
Laguerre	1.194×10^{-6}	2.200×10^{-24}	1.929×10^{-6}	6.096×10^{-8}	5.923

Table 3 The error distributions and the precision factor (scd) for Problem 1 with number of steps = 10^4

	<i>MaxErr</i>	<i>LastErr</i>	<i>Norm</i>	<i>RMSE</i>	<i>scd</i>
L-stable	1.057×10^{-12}	1.748×10^{-30}	6.423×10^{-12}	6.423×10^{-14}	11.98
RadaulIA	1.583×10^{-11}	3.931×10^{-23}	9.623×10^{-11}	9.623×10^{-13}	10.80
MHIRK	2.657×10^{-12}	4.406×10^{-30}	1.615×10^{-11}	1.615×10^{-13}	11.58
BSHM1	3.117×10^{-10}	4.300×10^{-28}	1.729×10^{-9}	1.729×10^{-11}	9.506
BSHM2	1.678×10^{-10}	7.159×10^{-25}	9.082×10^{-10}	9.081×10^{-12}	9.775
IRK	1.433×10^{-11}	1.667×10^{-20}	8.708×10^{-11}	8.707×10^{-13}	10.84
Radaul	1.611×10^{-11}	3.971×10^{-23}	9.790×10^{-11}	9.789×10^{-13}	10.79
Laguerre	2.436×10^{-12}	2.196×10^{-30}	6.537×10^{-12}	6.537×10^{-14}	11.61

Figure 3 Comparison of the \mathcal{L} -stable block method given in equation (11) with several other methods via efficiency curves of the absolute maximum global error versus CPU time (sec) for Problem 1 while matching the absolute maximum global error to the tolerance 10^{-i} under each method, where $i = 3, 6, 8$ (see online version for colours)



Problem 2: Consider another highly stiff IVP taken from Ramos and Rufai (2018):

$$v'(x) = -10^3v(x) + \exp(-2x), v(0) = 0, \tag{24}$$

whose exact solution is: $v(x) = \frac{1}{998}(\exp(-2x) - \exp(-10^3x))$.

The above stiff IVP is simulated over the integration interval $[0, 5]$ while taking different number of steps in powers of 10. The numerical results are shown in Tables 4–6 wherein computations for the accuracy and the precision factor are carried out with the proposed and several other methods. It can be seen that the proposed \mathcal{L} -stable method performs better in both directions, namely, smallest errors and highest precision factors are achieved with the method given in equation (11). The fifth-order accuracy is also observed from the behaviour of last absolute error since the powers of 10 decrease by magnitude 5 with every 1 order of magnitude increase in the powers of 10 in number of steps. Moreover, the efficiency curve given in Figure 4 reveals time-efficiency of the proposed \mathcal{L} -stable method wherein the method RadauIIA is, once again, observed to be the most expensive one.

Table 4 The error distributions and the precision factor (scd) for Problem 2 with number of steps = 10^2

	<i>MaxErr</i>	<i>LastErr</i>	<i>Norm</i>	<i>RMSE</i>	<i>scd</i>
L-stable	4.144×10^{-5}	9.657×10^{-21}	4.147×10^{-5}	4.127×10^{-6}	4.383
RadauIIA	4.267×10^{-5}	1.043×10^{-15}	4.271×10^{-5}	4.249×10^{-6}	4.370
MHIRK	1.858×10^{-5}	5.445×10^{-21}	1.858×10^{-5}	1.849×10^{-6}	4.731
BSHM1	1.915×10^{-4}	1.162×10^{-17}	2.591×10^{-4}	2.553×10^{-5}	3.718
BSHM2	1.526×10^4	1.526×10^4	1.964×10^4	1.935×10^3	-4.184
IRK	3.033×10^{260}	3.033×10^{260}	3.033×10^{260}	3.018×10^{259}	-260.50
RadauI	3.580×10^{104}	3.580×10^{104}	3.593×10^{104}	3.575×10^{103}	-104.60
Laguerre	7.182×10^{-4}	5.877×10^{-11}	1.049×10^{-3}	1.044×10^{-4}	3.144

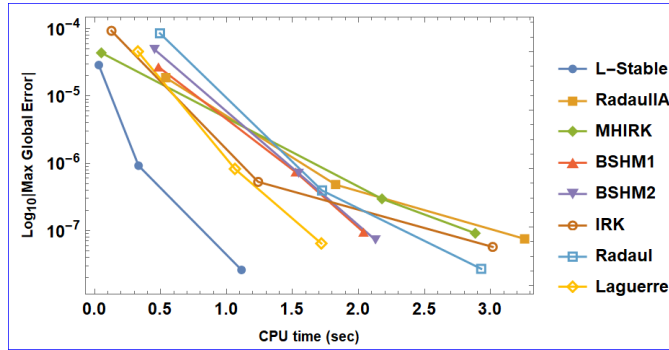
Table 5 The error distributions and the precision factor (scd) for Problem 2 with number of steps = 10^3

	<i>MaxErr</i>	<i>LastErr</i>	<i>Norm</i>	<i>RMSE</i>	<i>scd</i>
L-stable	9.228×10^{-7}	5.396×10^{-26}	9.228×10^{-7}	2.917×10^{-8}	6.035
RadauIIA	1.872×10^{-5}	2.482×10^{-19}	1.873×10^{-5}	5.921×10^{-7}	4.728
MHIRK	2.843×10^{-6}	1.048×10^{-25}	2.843×10^{-6}	8.987×10^{-8}	5.546
BSHM1	9.073×10^{-5}	3.078×10^{-23}	9.694×10^{-5}	3.061×10^{-6}	4.042
BSHM2	2.707×10^{-4}	9.567×10^{-20}	2.881×10^{-4}	9.097×10^{-6}	3.567
IRK	2.520×10^{-4}	$0. \times 10^{79}$	$0. \times 10^{79}$	$0. \times 10^{77}$	3.599
RadauI	8.534×10^{-5}	$0. \times 10^{136}$	$0. \times 10^{136}$	$0. \times 10^{135}$	4.069
Laguerre	4.583×10^{-5}	1.125×10^{-23}	4.765×10^{-5}	1.506×10^{-6}	4.339

Table 6 The error distributions and the precision factor (scd) for Problem 2 with number of steps = 10^4

	<i>MaxErr</i>	<i>LastErr</i>	<i>Norm</i>	<i>RMSE</i>	<i>scd</i>
L-stable	9.832×10^{-11}	7.826×10^{-31}	1.886×10^{-10}	1.886×10^{-12}	10.01
RadauIIA	1.485×10^{-9}	4.500×10^{-24}	2.850×10^{-9}	2.850×10^{-11}	8.828
MHIRK	2.631×10^{-10}	2.150×10^{-30}	5.047×10^{-10}	5.047×10^{-12}	9.580
BSHM1	5.678×10^{-8}	5.589×10^{-29}	6.374×10^{-8}	6.373×10^{-10}	7.246
BSHM2	4.131×10^{-8}	2.110×10^{-25}	5.933×10^{-8}	5.932×10^{-10}	7.384
IRK	1.809×10^{-9}	$0. \times 10^{95}$	$0. \times 10^{96}$	$0. \times 10^{94}$	8.743
RadauI	1.763×10^{-9}	$0. \times 10^{178}$	$0. \times 10^{333}$	$0. \times 10^{331}$	8.754
Laguerre	1.197×10^{-9}	1.057×10^{-29}	1.932×10^{-9}	1.932×10^{-11}	8.922

Figure 4 Comparison of the \mathcal{L} -stable block method given in equation (11) with several other methods via efficiency curves of the absolute maximum global error versus CPU time (sec) for Problem 2 while matching the absolute maximum global error to the tolerance 10^{-i} under each method, where $i = 5, 7, 8$ (see online version for colours)



Next, we consider stiff systems of two- and three-dimensions, and carry out the numerical simulations for the computations of different types of errors including infinity norm, root mean square error, absolute average error, and the precision factor denoted by *scd*. The number of steps chosen for every stiff system is chosen to be $n = 2^i$, where $i = 6, 8, 10$. It is observed from Tables 7–21 that the proposed \mathcal{L} -stable block method outperforms every other method under consideration in terms of not only accuracy but in the precision as well. The three fifth-order methods denoted by BSHM2, IRK and RadauI diverge in most of the cases thereby indicate the weak performance until a large number of steps are used. The \mathcal{L} -stable block method performs better than not only fifth-order methods but also produces smaller errors than the Laguerre method which is at least fifth-order. The efficiency curve in Figure 5 for the two-dimensional stiff system given in equation (25) is plotted to show computational time-efficiency of the proposed \mathcal{L} -stable block method while the same advantage has been observed for remaining stiff systems whose efficiency curves are not provided herein for the sake of brevity.

Problem 3: Consider the following two-dimensional stiff system taken from Nasarudin et al. (2020):

$$\begin{aligned} v_1'(x) &= 9v_1(x) + 24v_2(x) + 5 \cos(x) - \frac{1}{3} \sin(x), \quad v_1(0) = \frac{4}{3}, \\ v_2'(x) &= -24v_1(x) - 51v_2(x) - 9 \cos(x) + \frac{1}{3} \sin(t), \quad v_2(0) = \frac{2}{3}, \end{aligned} \tag{25}$$

where $t \in [0, 10]$. The exact solution of the stiff system (25) with stiffness ratio of 13 is as follows:

$$\begin{aligned} v_1(x) &= 2 \exp(-3x) - \exp(-39x) + \frac{1}{3} \cos(x), \\ v_2(x) &= -\exp(-3x) + 2 \exp(-39x) - \frac{1}{3} \cos(x). \end{aligned} \tag{26}$$

Table 7 The error distributions and the precision factor (scd) for Problem 3 with number of steps = 2^6

	$Norm_\infty$	$RMSE$	$Mean$	scd
L-stable	5.276×10^{-11}	4.079×10^{-11}	3.805×10^{-11}	2.274
RadauIIA	7.116×10^{-8}	5.905×10^{-8}	5.743×10^{-8}	1.558
MHIRK	1.510×10^{-10}	1.203×10^{-10}	1.147×10^{-10}	2.159
BSHM1	3.320×10^{-9}	2.362×10^{-9}	1.845×10^{-9}	0.656
BSHM2	2.002×10^{-7}	1.719×10^{-7}	1.690×10^{-7}	0.118
IRK	2.269×10^{-6}	1.793×10^{-6}	1.701×10^{-6}	-0.066
RadauI	8.434×10^{-8}	1.221×10^{-7}	1.175×10^{-7}	0.483
Laguerre	1.072×10^{-9}	1.061×10^{-9}	1.061×10^{-9}	0.823

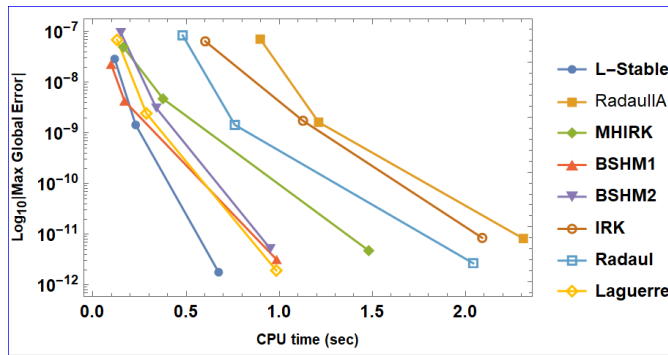
Table 8 The error distributions and the precision factor (scd) for Problem 3 with number of steps = 2^8

	$Norm_\infty$	$RMSE$	$Mean$	scd
L-stable	5.788×10^{-14}	4.641×10^{-14}	4.441×10^{-14}	4.436
RadauIIA	1.225×10^{-10}	9.956×10^{-11}	9.596×10^{-11}	3.489
MHIRK	1.491×10^{-13}	1.204×10^{-13}	1.156×10^{-13}	3.911
BSHM1	1.173×10^{-11}	9.173×10^{-12}	8.637×10^{-12}	1.891
BSHM2	1.210×10^{-10}	1.057×10^{-10}	1.043×10^{-10}	1.770
IRK	1.744×10^{-9}	1.379×10^{-9}	1.308×10^{-9}	2.825
RadauI	9.007×10^{-11}	1.318×10^{-10}	1.267×10^{-10}	2.965
Laguerre	2.456×10^{-13}	2.440×10^{-13}	2.440×10^{-13}	2.965

Table 9 The error distributions and the precision factor (scd) for Problem 3 with number of steps = 2^{10}

	$Norm_{\infty}$	RMSE	Mean	scd
L-stable	5.767×10^{-17}	4.653×10^{-17}	4.468×10^{-17}	7.293
RadauIIA	1.359×10^{-13}	1.102×10^{-13}	1.060×10^{-13}	6.417
MHIRK	1.452×10^{-16}	1.173×10^{-16}	1.127×10^{-16}	6.873
BSHM1	1.441×10^{-14}	1.149×10^{-14}	1.096×10^{-14}	4.545
BSHM2	6.279×10^{-14}	5.967×10^{-14}	5.959×10^{-14}	4.735
IRK	1.430×10^{-12}	1.131×10^{-12}	1.073×10^{-12}	6.065
RadauI	8.136×10^{-14}	1.184×10^{-13}	1.139×10^{-13}	6.060
Laguerre	5.948×10^{-17}	5.887×10^{-17}	5.887×10^{-17}	6.337

Figure 5 Comparison of the \mathcal{L} -stable block method given in equation (11) with several other methods via efficiency curves of the absolute maximum global error versus CPU time (sec) for Problem 3 while matching the absolute maximum global error to the tolerance 10^{-i} under each method, where $i = 8, 9, 12$ (see online version for colours)



Problem 4: Consider the following oscillatory stiff problem used in physics as the torsion spring oscillator (Rufai and Ramos, 2020):

$$\begin{aligned}
 v_1'(x) &= 998v_1(x) + 1,998v_2(x), \\
 v_2'(x) &= -999v_1(x) - 1,999v_2(x), \\
 v_1(0) &= 1, \quad v_2(0) = 2, \quad t \in [0, 5].
 \end{aligned}
 \tag{27}$$

Analytical solution is: $v_1(x) = -5 \exp(-10^3x) + 6 \exp(-x)$, $v_2(x) = 5 \exp(-10^3x) - 3 \exp(-x)$.

Problem 5: The sinusoidal stiff system taken from Akinfenwa et al. (2020) is given below:

$$\begin{aligned}
 v_1'(x) &= -2v_1(x) + v_2(x) + 2 \sin(x), \\
 v_2'(x) &= 998v_1(x) - 999v_2(x) + 999 \cos(x) - 999 \sin(x), \\
 v_1(0) &= 2, \quad v_2(0) = 3, \quad t \in [0, 2].
 \end{aligned}
 \tag{28}$$

Analytical solution is: $v_1(x) = 2 \exp(-x) + \sin(x)$, $v_2(x) = 2 \exp(-x) + \cos(x)$.

Table 10 The error distributions and the precision factor (scd) for Problem 4 with number of steps = 2^6

	$Norm_\infty$	$RMSE$	$Mean$	scd
L-stable	5.385×10^{-12}	4.257×10^{-12}	4.039×10^{-12}	26.240
RadauIIA	8.064×10^{-11}	6.375×10^{-11}	6.048×10^{-11}	23.530
MHIRK	1.359×10^{-11}	1.074×10^{-11}	1.019×10^{-11}	25.310
BSHM1	1.124×10^{-9}	8.885×10^{-10}	8.429×10^{-10}	20.89
BSHM2	1.142×10^6	1.142×10^6	1.142×10^6	-13.950
IRK	1.368×10^{199}	1.368×10^{199}	1.368×10^{199}	-458.5
RadauI	1.943×10^{85}	1.943×10^{85}	1.943×10^{85}	-196.4
Laguerre	5.436×10^{-3}	5.436×10^{-3}	5.436×10^{-3}	5.215

Table 11 The error distributions and the precision factor (scd) for Problem 4 with number of steps = 2^8

	$Norm_\infty$	$RMSE$	$Mean$	scd
L-stable	5.304×10^{-15}	4.194×10^{-15}	3.978×10^{-15}	33.160
RadauIIA	7.953×10^{-14}	6.287×10^{-14}	5.965×10^{-14}	30.450
MHIRK	1.329×10^{-14}	1.051×10^{-14}	9.969×10^{-15}	32.240
BSHM1	1.344×10^{-12}	1.062×10^{-12}	1.008×10^{-12}	27.620
BSHM2	7.092×10^6	7.092×10^6	7.092×10^6	-15.77
IRK	5.073×10^{397}	5.073×10^{397}	5.073×10^{397}	-915.8
RadauI	$0. \times 10^{162}$	$0. \times 10^{162}$	$0. \times 10^{162}$	1
Laguerre	2.227×10^{-15}	1.760×10^{-15}	1.670×10^{-15}	34.030

Table 12 The error distributions and the precision factor (scd) for Problem 4 with number of steps = 2^{10}

	$Norm_\infty$	$RMSE$	$Mean$	scd
L-stable	5.191×10^{-18}	4.104×10^{-18}	3.893×10^{-18}	0.409
RadauIIA	7.786×10^{-17}	6.155×10^{-17}	5.839×10^{-17}	0.373
MHIRK	1.299×10^{-17}	1.027×10^{-17}	9.739×10^{-18}	0.391
BSHM1	1.379×10^{-15}	1.091×10^{-15}	1.035×10^{-15}	0.345
BSHM2	7.071×10^{-16}	5.590×10^{-16}	5.303×10^{-16}	0.3517
IRK	$0. \times 10^{268}$	$0. \times 10^{268}$	$0. \times 10^{268}$	1
RadauI	$0. \times 10^{384}$	$0. \times 10^{384}$	$0. \times 10^{384}$	1
Laguerre	5.436×10^{-19}	4.297×10^{-19}	4.077×10^{-19}	0.423

Table 13 The error distributions and the precision factor (scd) for Problem 5 with number of steps = 2^6

	$Norm_\infty$	$RMSE$	$Mean$	scd
L-stable	5.267×10^{-14}	5.241×10^{-14}	5.241×10^{-14}	12.850
RadauIIA	3.938×10^{-10}	2.785×10^{-10}	2.005×10^{-10}	11.130
MHIRK	1.320×10^{-13}	1.319×10^{-13}	1.319×10^{-13}	12.450
BSHM1	1.538×10^{-11}	1.516×10^{-11}	1.516×10^{-11}	10.390
BSHM2	1.404×10^{-6}	9.929×10^{-7}	7.028×10^{-7}	5.853
IRK	2.191×10^{128}	1.549×10^{128}	1.097×10^{128}	-12.83
RadauI	7.531×10^{37}	5.315×10^{40}	3.762×10^{40}	-40.88
Laguerre	2.275×10^{-13}	1.669×10^{-13}	1.453×10^{-13}	12.510

Table 14 The error distributions and the precision factor (scd) for Problem 5 with number of steps = 2^8

	$Norm_\infty$	$RMSE$	$Mean$	scd
L-stable	5.130×10^{-17}	5.106×10^{-17}	5.106×10^{-17}	15.860
RadauIIA	2.859×10^{-12}	2.021×10^{-12}	1.434×10^{-12}	14.020
MHIRK	1.274×10^{-16}	1.273×10^{-16}	1.273×10^{-16}	15.460
BSHM1	1.417×10^{-14}	1.407×10^{-14}	1.407×10^{-14}	13.420
BSHM2	5.256×10^{-13}	3.736×10^{-13}	2.897×10^{-13}	11.900
IRK	3.248×10^{42}	2.297×10^{42}	1.626×10^{42}	-42.510
RadauI	$0. \times 10^2$	$0. \times 10^4$	$0. \times 10^2$	1
Laguerre	5.891×10^{-17}	4.305×10^{-17}	3.715×10^{-17}	16.070

Table 15 The error distributions and the precision factor (scd) for Problem 5 with number of steps = 2^{10}

	$Norm_\infty$	$RMSE$	$Mean$	scd
L-stable	4.961×10^{-20}	4.953×10^{-20}	4.953×10^{-20}	18.870
RadauIIA	6.220×10^{-15}	4.398×10^{-15}	3.116×10^{-15}	16.890
MHIRK	1.241×10^{-19}	1.237×10^{-19}	1.237×10^{-19}	18.470
BSHM1	1.351×10^{-17}	1.348×10^{-17}	1.348×10^{-17}	16.440
BSHM2	2.067×10^{-16}	1.507×10^{-16}	1.294×10^{-16}	15.360
IRK	$0. \times 10^{-7}$	$0. \times 10^{-7}$	$0. \times 10^{-10}$	11.310
RadauI	$0. \times 10^{20}$	$0. \times 10^{22}$	$0. \times 10^{20}$	2
Laguerre	1.365×10^{-20}	1.001×10^{-20}	8.704×10^{-21}	19.660

Problem 6: Consider the following highly stiff three-dimensional linear system mentioned in Sahi et al. (2012):

$$\begin{aligned}
 v_1'(x) &= -21v_1(x) + 19v_2(x) - 20v_3(x), \\
 v_2'(x) &= 19v_1(x) - 21v_2(x) + 20v_3(x), \\
 v_3'(x) &= 40v_1(x) - 40v_2(x) + 40v_3(x), \\
 v_1(0) &= 1, \quad v_2(0) = 0, \quad v_3(0) = -1, \quad t \in [0, 1].
 \end{aligned}
 \tag{29}$$

The exact solution is available as:

$$v_1(x) = \frac{1}{2} \left(\exp(-2x) + \exp(-40x) (\cos(40x) + \sin(40x)) \right),$$

$$v_2(x) = \frac{1}{2} \left(\exp(-2x) - \exp(-40x) (\cos(40x) + \sin(40x)) \right),$$

$$v_3(x) = \frac{1}{2} \left(2 \exp(-40x) (\sin(40x) - \cos(40x)) \right).$$

Table 16 The error distributions and the precision factor (scd) for Problem 6 with number of steps = 2^6

	$Norm_\infty$	RMSE	Mean	scd
L-stable	3.718×10^{-14}	3.035×10^{-14}	2.478×10^{-14}	5.515
RadauIIA	5.572×10^{-13}	4.550×10^{-13}	3.715×10^{-13}	4.348
MHIRK	9.328×10^{-14}	7.616×10^{-14}	6.219×10^{-14}	5.091
BSHM1	9.229×10^{-12}	7.535×10^{-12}	6.153×10^{-12}	2.813
BSHM2	5.396×10^{-12}	4.406×10^{-12}	3.597×10^{-12}	2.790
IRK	4.979×10^{-13}	4.065×10^{-13}	3.319×10^{-13}	4.196
RadauI	5.632×10^{-13}	4.599×10^{-13}	3.755×10^{-13}	4.246
Laguerre	2.501×10^{-14}	2.042×10^{-14}	1.668×10^{-14}	4.217

Table 17 The error distributions and the precision factor (scd) for Problem 6 with number of steps = 2^8

	$Norm_\infty$	RMSE	Mean	scd
L-stable	3.643×10^{-17}	2.974×10^{-17}	2.429×10^{-17}	8.463
RadauIIA	5.463×10^{-16}	4.461×10^{-16}	3.642×10^{-16}	7.288
MHIRK	9.116×10^{-17}	7.443×10^{-17}	6.077×10^{-17}	8.055
BSHM1	9.633×10^{-15}	7.865×10^{-15}	6.422×10^{-15}	5.894
BSHM2	5.012×10^{-15}	4.092×10^{-15}	3.341×10^{-15}	6.117
IRK	4.805×10^{-16}	3.924×10^{-16}	3.204×10^{-16}	7.295
RadauI	5.478×10^{-16}	4.473×10^{-16}	3.652×10^{-16}	7.261
Laguerre	6.106×10^{-18}	4.985×10^{-18}	4.070×10^{-18}	7.734

Table 18 The error distributions and the precision factor (scd) for Problem 6 with number of steps = 2^{10}

	$Norm_\infty$	RMSE	Mean	scd
L-stable	3.561×10^{-20}	2.907×10^{-20}	2.374×10^{-20}	11.460
RadauIIA	5.341×10^{-19}	4.361×10^{-19}	3.560×10^{-19}	10.290
MHIRK	8.903×10^{-20}	7.270×10^{-20}	5.936×10^{-20}	11.060
BSHM1	9.564×10^{-18}	7.809×10^{-18}	6.376×10^{-18}	9.000
BSHM2	4.830×10^{-18}	3.943×10^{-18}	3.220×10^{-18}	9.270
IRK	4.679×10^{-19}	3.820×10^{-19}	3.119×10^{-19}	10.330
RadauI	5.344×10^{-19}	4.363×10^{-19}	3.563×10^{-19}	10.280
Laguerre	1.491×10^{-21}	1.217×10^{-21}	9.937×10^{-22}	11.310

Table 19 The error distributions and the precision factor (scd) for Problem 7 with number of steps = 2^6

	$Norm_\infty$	$RMSE$	$Mean$	scd
L-stable	7.435×10^{-14}	4.293×10^{-14}	2.478×10^{-14}	1.129
RadauIIA	1.114×10^{-12}	6.434×10^{-13}	3.715×10^{-13}	0.945
MHIRK	1.866×10^{-13}	1.077×10^{-13}	6.219×10^{-14}	1.581
BSHM1	1.846×10^{-11}	1.066×10^{-11}	6.153×10^{-12}	0.448
BSHM2	9.767×10^3	5.639×10^3	3.257×10^3	-3.990
IRK	1.721×10^{149}	9.937×10^{148}	5.737×10^{148}	-14.92
RadauI	3.820×10^{16}	3.293×10^{57}	1.901×10^{57}	-57.76
Laguerre	6.811×10^{-7}	3.932×10^{-7}	2.270×10^{-7}	0.005

Table 20 The error distributions and the precision factor (scd) for Problem 7 with number of steps = 2^8

	$Norm_\infty$	$RMSE$	$Mean$	scd
L-stable	7.286×10^{-17}	4.206×10^{-17}	2.429×10^{-17}	1.922
RadauIIA	1.093×10^{-15}	6.308×10^{-16}	3.642×10^{-16}	1.229
MHIRK	1.823×10^{-16}	1.053×10^{-16}	6.077×10^{-17}	2.462
BSHM1	1.927×10^{-14}	1.112×10^{-14}	6.422×10^{-15}	0.678
BSHM2	1.002×10^{-14}	5.826×10^{-15}	3.730×10^{-15}	0.079
IRK	9.870×10^{126}	5.699×10^{126}	3.290×10^{126}	-12.70
RadauI	$0. \times 10^{12}$	$0. \times 10^{22}$	$0. \times 10^{12}$	0
Laguerre	1.221×10^{-17}	7.050×10^{-18}	4.070×10^{-18}	0.701

Table 21 The error distributions and the precision factor (scd) for Problem 7 with number of steps = 2^{10}

	$Norm_\infty$	$RMSE$	$Mean$	scd
L-stable	7.121×10^{-20}	4.111×10^{-20}	2.374×10^{-20}	4.099
RadauIIA	1.068×10^{-18}	6.167×10^{-19}	3.560×10^{-19}	2.711
MHIRK	1.781×10^{-19}	1.028×10^{-19}	5.936×10^{-20}	3.432
BSHM1	1.913×10^{-17}	1.104×10^{-17}	6.376×10^{-18}	1.616
BSHM2	9.660×10^{-18}	5.577×10^{-18}	3.220×10^{-18}	1.385
IRK	$0. \times 10^7$	$0. \times 10^7$	$0. \times 10^3$	0
RadauI	$0. \times 10^{20}$	$0. \times 10^{45}$	$0. \times 10^{20}$	0
Laguerre	2.981×10^{-21}	1.721×10^{-21}	9.937×10^{-22}	2.438

Problem 7: Finally, we consider another three-dimensional linear stiff system discussed in Wu (1998):

$$\begin{aligned}
 v_1'(x) &= -0.1v_1(x) - 49.9v_2(x), \quad v_2'(x) = 50v_2, \\
 v_3'(x) &= 70v_2(x) + 120v_3(x), \\
 v_1(0) &= 2, \quad v_2(0) = 1, \quad v_3(0) = 2, \quad x \in [0, 20].
 \end{aligned}
 \tag{30}$$

The exact solution is available as: $v_1(x) = \exp(-50x) + \exp(-0.1x)$, $v_2(x) = \exp(-50x)$, $v_3(x) = \exp(-50x) + \exp(-120x)$.

5 Concluding remarks with future plans

In this paper, a new family of block methods with robust \mathcal{L} -stability characteristics for the numerical solution of IVPs of stiff differential equations with different nature has been constructed efficiently. At the same time, the main computations are carried out with one of the family members for a suitable choice of the two intra-step points. From the analysis of the properties, the proposed method was consistent, linearly stable, zero-stable, and thus convergent. Furthermore, the relative measure of stability (order stars) was carried out to identify the poles. Highly stiff differential equations of different characteristics were solved via the proposed and other existing methods, while the former performed far better in accuracy and efficiency. The methodology can further be applied to nonlinear, highly stiff delay differential models emanated from real-life situations. Finally, the approaches will be devised in the future to obtain an optimal member of the proposed \mathcal{L} -stable family.

References

- Abdulganiy, R.I., Akinfenwa, O.A., Ramos, H. and Okunuga, S.A. (2021) 'A second-derivative functionally fitted method of maximal order for oscillatory initial value problems', *Computational and Applied Mathematics*, Vol. 40, No. 6, p.128.
- Achchab, B., Abda, A. and Sakat, A. (2020) 'Stopping criteria based on the reciprocity gap concept for data boundary recovering', *Applied and Computational Mathematics*, Vol. 19, No. 3, pp.283–299.
- Ajayi, S.A., Muka, K.O. and Ibrahim, O.M. (2019) 'A family of stiffly stable second-derivative block methods for initial value problems in ordinary differential equations', *Earthline Journal of Mathematical Sciences*, Vol. 1, No. 2, pp.2581–8147.
- Akinfenwa, O.A., Abdulganiy, R.I., Akinnukawe, B.I. and Okunuga, S.A. (2020) 'Seventh order hybrid block method for solution of first order stiff systems of initial value problems', *Journal of the Egyptian Mathematical Society*, Vol. 28, No. 1, pp.1–11.
- Akinfenwa, O.A., Okunuga, S.A., Akinnukawe, B.I., Rufai, U.P. and Abdulganiy, R.I. (2018) 'Multi-derivative hybrid implicit Runge-Kutta method for solving stiff system of a first order differential equation', *Far East Journal of Mathematical Sciences (FJMS)*, Vol. 106, No. 2, pp.543–562.
- Aliev, F.A., Aliev, N.A., Safarova, N.A. and Mamedova, Y.V. (2021) 'Solution of the problem of analytical construction of optimal regulators for a fractional order oscillatory system in the general case', *Journal of Applied and Computational Mechanics*, Vol. 7, No. 2, pp.970–976.
- Aliev, F.A., Aliev, N.A., Velieva, N.I. and Safarova, N.A. (2020) 'Larin parameterization to solve the problem of analytical construction of the optimal regulator of oscillatory systems with liquid dampers', *Journal of Applied and Computational Mechanics*, Vol. 6, pp.1426–1430, Special issue.
- Argyros, I.K. and George, S. (2021) 'Extended Kung-Traub-type method for solving equations', *TWMS Journal of Pure and Applied Mathematics*, Vol. 12, No. 2, pp.193–198.
- Ashyralyev, A., Agirseven, D. and Agarwal, R.P. (2020) 'Stability estimates for delay parabolic differential and difference equations', *Appl. Comput. Math*, Vol. 19, No. 2, pp.175–204.
- Awari, Y.S., Shikaa, S. and Stephen, N.M. (2020) 'A family of second-derivative Simpson's type block methods for stiff systems', *Journal of Advance Research in Mathematics and Statistics*, Vol. 7, No. 9, pp.1–22.
- Awoyemi, D.O. (2001) 'A new sixth-order algorithm for general second order ordinary differential equations', *International Journal of Computer Mathematics*, Vol. 77, No. 1, pp.117–124.

- Bavi, R., Hajnayeb, A., Sedighi, H.M. and Shishesaz, M. (2022) ‘Simultaneous resonance and stability analysis of unbalanced asymmetric thin-walled composite shafts’, *International Journal of Mechanical Sciences*, Vol. 217, No. 1, p.107047.
- Butcher, J.C. (2016) *Numerical Methods for Ordinary Differential Equations*, John Wiley & Sons, The Atrium, Southern Gate, Chichester, West Sussex, P.O. 19 8SQ, UK.
- Fadugba, S.E. (2020) ‘Development of an improved numerical integration method via the transcendental function of exponential form’, *Journal of Interdisciplinary Mathematics*, Vol. 23, No. 7, pp.1347–1356 [online] <https://doi.org/10.1080/09720502.2020.1747196>.
- Gao, X.Y., Guo, Y.J. and Shan, W.R. (2021) ‘Similarity reductions for a $(3 + 1)$ -dimensional generalized Kadomtsev-Petviashvili equation in nonlinear optics, fluid mechanics and plasma physics’, *Applied and Computational Mathematics*, Vol. 20, No. 3, pp.421–429.
- Gragg, W.B. and Stetter, H.J. (1964) ‘Generalized multistep predictor-corrector methods’, *Journal of the ACM (JACM)*, Vol. 11, No. 2, pp.188–209.
- Hairer, E., Nørsett, S.P. and Wanner, G. (1993) *Solving Ordinary Differential Equations. 1, Nonstiff Problems*, Springer-Vlg, Berlin, Heidelberg, New York.
- Hairer, E., Nørsett, S.P. and Wanner, G. (2008) *Solving Ordinary Differential Equations I, Nonstiff Problems*, Corr. 3rd printing, Springer, Berlin, Heidelberg.
- Henrici, P. (1962) *Discrete Variable Methods in Ordinary Differential Equations*, Wiley, New York.
- Heydari, M., Avazzadeh, Z. and Hosseinzadeh, N. (2020) ‘Haar wavelet method for solving high-order differential equations with multi-point boundary conditions’, *J. Appl. Comput. Mech.*, Vol. 8, No. 2, pp.528–544, DOI: 10.22055/JACM.2020.31860.1935.
- Isgendarov, N.S., Mehraliyev, Y.T. and Huseyinova, A.F. (2016) ‘On an inverse boundary value problem for the Boussinesq-Love equation with an integral condition’, *Applied Mathematical Sciences*, Vol. 10, No. 63, pp.3119–3131, DOI: 10.12988/ams.2016.6264.
- Jena, S.K., Chakraverty, S., Mahesh, V., Harursampath, D. and Sedighi, H.M. (2022) ‘A novel numerical approach for the stability of nanobeam exposed to hygro-thermo-magnetic environment embedded in elastic foundation’, *ZAMM – Journal of Applied Mathematics and Mechanics/Zeitschrift für Angewandte Mathematik und Mechanik*, Vol. 102, No. 5, p.e202100380.
- Kandasamy, P., Gunavathy, K. and Thilagavathy, K. (2005) *Engineering Mathematics, Volume I & II*, S. Chand and Company, New Delhi.
- Khalsaraei, M.M. and Shokri, A. (2020) ‘The new classes of high order implicit six-step P-stable multiderivative methods for the numerical solution of Schrodinger equation’, *Applied and Computational Mathematics*, Vol. 19, No. 1, pp.59–86.
- Kumar, A. and Verma, S.R. (2021) ‘Modified Taylor wavelets approach to the numerical results of second order differential equations’, *International Journal of Applied Nonlinear Science*, Vol. 3, No. 2, pp.136–155.
- Lambert, J.D. (1973) *Computational Methods in Ordinary Differential Equations*, John Wiley & Sons, Chichester, New York.
- Lambert, J.D. (1991) *Numerical Methods for Ordinary Differential Systems*, Vol. 146, Wiley, New York.
- Mostafa, A.O. and El Hawsh, G.M. (2020) ‘Differential subordination applications to a class of p -valent functions associated with Mittag-Leffler function’, *Proceedings of the Institute of Applied Mathematics*, Vol. 9, No. 1, pp.46–59.
- Musaev, H.K. (2021) ‘The Cauchy problem for degenerate parabolic convolution equation’, *TWMS Journal of Pure and Applied Mathematics*, Vol. 12, No. 2, pp.278–288.
- Nasarudin, A.A., Ibrahim, Z.B. and Rosali, H. (2020) ‘On the integration of stiff ODEs using block backward differentiation formulas of order six’, *Symmetry*, Vol. 12, No. 6, p.952.
- Onyejekwe, O.O. (2018). A hybrid numerical treatment of nonlinear reaction-diffusion equations with memory: a prototypical Fisher-Kolmogorov-Petrovskii-Piskunov equation’, *International Journal of Applied Nonlinear Science*, Vol. 3, No. 1, pp.1–20.

- Qureshi, S. and Ramos, H. (2018) 'L-stable explicit nonlinear method with constant and variable step-size formulation for solving initial value problems', *International Journal of Nonlinear Sciences and Numerical Simulation*, Vol. 19, Nos. 7–8, pp.741–751.
- Qureshi, S. and Yusuf, A. (2020) 'A new third order convergent numerical solver for continuous dynamical systems', *Journal of King Saud University-Science*, Vol. 32, No. 2, pp.1409–1416.
- Qureshi, S., Soomro, A. and Hinçal, E. (2021) 'A new family of A-acceptable nonlinear methods with fixed and variable stepsize approach', *Computational and Mathematical Methods*, Vol. 3, No. 6, p.e1213.
- Ramos, H. (2017) 'An optimized two-step hybrid block method for solving first-order initial-value problems in ODEs', *Differential Geometry – Dynamical Systems*, Vol. 19, pp.107–118.
- Ramos, H. and Rufai, M.A. (2018) 'Third derivative modification of k-step block Falkner methods for the numerical solution of second order initial-value problems', *Applied Mathematics and Computation*, Vol. 333, pp.231–245.
- Ramos, H. and Rufai, M.A. (2020) 'A two-step hybrid block method with fourth derivatives for solving third-order boundary value problems', *Journal of Computational and Applied Mathematics*, Article in press.
- Ramos, H. and Vigo-Aguiar, J. (2007) 'An almost L-stable BDF-type method for the numerical solution of stiff ODEs arising from the method of lines', *Numerical Methods for Partial Differential Equations*, Vol. 20, No. 5, pp.1110–1121.
- Ramos, H., Qureshi, S. and Soomro, A. (2021) 'Adaptive step-size approach for Simpson's-type block methods with time efficiency and order stars', *Computational and Applied Mathematics*, Vol. 40, No. 6, pp.1–20.
- Rao, N.S. and Kalyani, K. (2021) 'Fixed point theorems for the extensions of Pandhare and Waghmode in Hilbert space', *Proceedings of IAM*, Vol. 10, No. 1, pp.3–15.
- Rufai, M.A. and Ramos, H. (2020) 'One-step hybrid block method containing third derivatives and improving strategies for solving Bratu's and Troesch's problems', *Numerical Mathematics: Theory, Methods & Applications*, Vol. 13, No. 4, pp.946–972.
- Rufai, M.A., Duromola, M.K. and Ganiyu, A.A. (2016) 'Derivation of one-sixth hybrid block method for solving general first order ordinary differential equations', *IOSR-JM*, Vol. 12, No. 5, pp.20–27.
- Sahi, R.K., Jator, S.N. and Khan, N.A. (2012) 'A Simpson's-type second-derivative method for stiff systems', *International Journal of Pure and Applied Mathematics*, Vol. 81, No. 4, pp.619–633.
- See, P.P., Majid, Z.A. and Suleiman, M. (2014) 'Three-step block method for solving nonlinear boundary value problems', *Abstract and Applied Analysis*, Vol. 2014, Article ID 379829, 8pp [online] <http://dx.doi.org/10.1155/2014/379829>.
- Shokri, A., Vigo-Aguiar, J., Khalsaraei, M.M. and Garcia-Rubio, R. (2020) 'A new implicit six-step P-stable method for the numerical solution of Schrödinger equation', *International Journal of Computer Mathematics*, Vol. 97, No. 4, pp.802–817.
- Shokri, A., Khalsaraei, M.M. and Atashyar, A. (2020) 'A new two-step hybrid singularly P-stable method for the numerical solution of second-order IVPs with oscillating solutions', *Iranian Journal of Mathematical Chemistry*, Vol. 11, No. 2, pp.113–132.
- Singla, R., Singh, G., Kanwar, V. and Ramos, H. (2021) 'Efficient adaptive step-size formulation of an optimized two-step hybrid block method for directly solving general second-order initial-value problems', *Computational and Applied Mathematics*, Vol. 40, p.220 [online] <https://doi.org/10.1007/s40314-021-01599-z>.
- Skwame, Y., Sunday, J. and Ibijola, E.A. (2012) 'L-stable block hybrid Simpson's methods for numerical solution of initial value problems in stiff ordinary differential equations', *International Journal of Pure and Applied Sciences and Technology*, Vol. 11, No. 2, p.45.

- Sunday, J., Kolawole, F.M., Ibijola, E.A. and Ogunrinde, R.B. (2015) ‘Two-step Laguerre polynomial hybrid block method for stiff and oscillatory first-order ordinary differential equations’, *J. Math. Comput. Sci.*, Vol. 5, No. 5, pp.658–668.
- Wanner, G. and Hairer, E. (1996) *Solving Ordinary Differential Equations II*, Springer, Berlin, Heidelberg, Germany.
- Wu, X.Y. (1998) ‘A sixth-order A-stable explicit one-step method for stiff systems’, *Computers & Mathematics with Applications*, Vol. 35, No. 9, pp.59–64.
- Yu, Y. (2004) *Stiff Problems in Numerical Simulation of Biochemical and Gene Regulatory Networks*, Doctoral dissertation, University of Georgia.

Appendix

Algorithm 1 Pseudo-code for the proposed one-step \mathcal{L} -stable block method

Data: x_0, X_N (integration interval), N (number of steps), v_{00}, v_{10}, v_{20} ,
(initial values), $g, \frac{dg}{dx}$

Result: **sol** (discrete approximate solution of the IVP (1))

- 1 Let $n = 0, \Delta x = \frac{X_N - x_0}{N}$
- 2 Let $x_n = x_0, v_n = v_{00}, v'_n = v_{10}, v''_n = v_{20}$
- 3 Let **sol** = $\{(x_n, v_n)\}$.
- 4 Solve equation (11) to obtain $v_{n+k}, v'_{n+k}, v''_{n+k}$, where $k = 0, r, s, 1$
- 5 Let **sol** = **sol** $\cup \{(x_{n+k}, v_{n+k})\}_{k=0,r,s,1}$
- 6 Let $x_n = x_n + \Delta x, v_n = v_{n+1}, v'_n = v'_{n+1}, v''_n = v''_{n+1}$
- 7 Let $n = n + 1$
- 8 **if** $n = N$ **then**
- 9 | go to 13
- 10 **else**
- 11 | go to 4;
- 12 **End**
